

Erythrocyte Destruction under Periodically Fluctuating Shear Rate: Comparative Study with Constant Shear Rate

Shigehiro Hashimoto

School of Medicine, Kitasato University, Sagamihara, Japan

Abstract: The hydrodynamic effect of periodically fluctuating shear rate on erythrocyte destruction was quantitatively studied *in vitro* in comparison with constant shear rates. Uniform shear rates ($<1,000 \text{ s}^{-1}$; constant or sinusoidally fluctuating with time) were applied to heparinized canine blood contained in the concavo-convex type of Couette flow testing machine for $(1.8-9.0) \times 10^3 \text{ s}$ at 24°C . The results show that the erythrocyte destruction

(evaluated with hemolysis ratio; plasma hemoglobin count per whole blood hemoglobin count) decreases when the exposure time of larger ($>500 \text{ s}^{-1}$) shear rates is interspersed with smaller ($<300 \text{ s}^{-1}$) shear rates. **Key Words:** Erythrocyte destruction—Hydrodynamic effect—Shear rate—Pulsatile flow—Concavo-convex testing machine—Couette flow.

In pulsatile flows (e.g., in arteries or in flow paths of the extracorporeal circulation with a pulsatile pump), blood is exposed to periodically fluctuating shear rates. To study quantitatively mechanical erythrocyte destruction in the pulsatile flow, the hydrodynamic effect of shear rates in a periodically fluctuating mode on erythrocyte destruction was studied in comparison with those in the constant mode *in vitro*.

MATERIALS AND METHODS

Three sets of the concavo-convex test system (Fig. 1) were manufactured in order to apply uniform shear rates to blood in Couette-type flow. A heparinized sample (hematocrit 38–45%) of beagle blood was filled between a stationary convex circular cone (diameter, 48 mm) and a rotating concave circular cone (rotated by DC motor; Sawamura Denki, Japan), and was sheared for $(1.8-9.0) \times 10^3 \text{ s}$ at 24°C . The concave (outer) part was rotated in order to minimize the effect of secondary flow

(Taylor vortex) (1) in the blood. Both cones (Fig. 2) are made of transparent polymethylmethacrylate, which enables the blood sample to be observed during tests. Their surface roughnesses measured by a stylus are in the order of $1 \mu\text{m}$. In order to evaluate the effect of surface-to-volume ratio ($1.6-6.3 \text{ mm}^{-1}$) on erythrocyte destruction, variations ($1.1^\circ-3.9^\circ$) were made in the angle between the convex and concave cones, namely, five convex cones (apex angle, $113.0^\circ-115.0^\circ$) and three concave cones (apex angle, $117.2^\circ-120.8^\circ$) were prepared. To prevent the blood sample from evaporation during tests, the concavo-convex test part was contained in polymethylmethacrylate chamber, in which the aqueous vapor was saturated. In this concavo-convex type testing machine, the uniform shear rates (G), which are calculated by Eq. 1, are applied in a similar way to a cone-and-plate type (Fig. 3) (2).

$$G = (6n/\phi) \sin(\alpha/2) \quad (1)$$

where n is the rotating speed (min^{-1}) of the concave cone, α is its apex angle, and ϕ is the angle ($^\circ$) between the convex and concave cones.

In any combination of the convex and concave cones, these shear rates, which are controlled in proportion to the rotating speed ($<350 \text{ min}^{-1}$) of the concave cone by a function generator (National, Japan), were periodically fluctuated with various

Received December 1987; revised November 1988.
Address correspondence and reprint requests to Shigehiro Hashimoto, Bioengineering, School of Medicine, Kitasato University, 15-1, Kitasato 1-chome, Sagamihara-shi, 228 Kanagawa, Japan.

This work was presented in part at the VIth World Congress of the International Society for Artificial Organs and XIVth Congress of the European Society for Artificial Organs.



FIG. 1. Test system. Left, concavo-convex testing machine; rotating-speed controller; right, function generator.

fluctuating conditions; the maximum (G_{\max}) ($<1,000 \text{ s}^{-1}$) or the minimum (G_{\min}) ($>0 \text{ s}^{-1}$) of shear rates and the frequency of fluctuation ($<0.8 \text{ Hz}$) in a sinusoidal mode (Fig. 4B). To compare with this sinusoidal mode, constant (Fig. 4A) and intermittent (Fig. 4C) modes were also tested. The variation of the rotating speed was measured by a tachometer. With the simultaneous use of three sets of test systems, every serial test (for which data is compared in Fig. 5A–F) was finished within 6 h of the blood drawing. Evaluation of erythrocyte destruction was derived from the hemolysis ratio (HR), which is calculated by

$$\text{HR} = R P_{\text{Hb}}/W_{\text{Hb}} \quad (2)$$

where R is the volumetric ratio of plasma to whole blood, P_{Hb} is the plasma hemoglobin concentration, and W_{Hb} is the whole blood hemoglobin concentration. The values of R and P_{Hb} were measured after centrifugation of blood for 10 min by $1.6 \times 10^3 g$ (g : acceleration of gravity). When all the hemoglobins are released from erythrocytes, HR becomes unity.

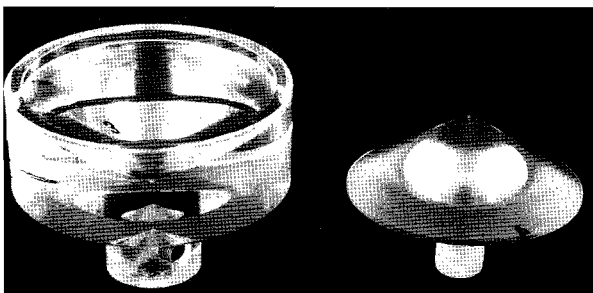


FIG. 2. Concave circular cone (left), and convex circular cone (right).

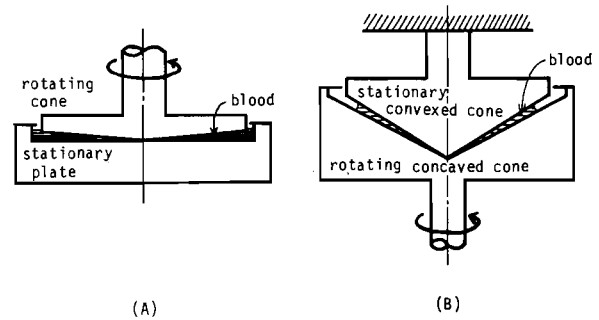


FIG. 3. Cone-plate (A) and concavo-convex (B) test equipments.

RESULTS

For 6 hours from the blood drawing, HR without shear in the concavo-convex type testing machine is $<5 \times 10^{-4}$, which is ignored in the following results. Data in sinusoidally fluctuating shear rates are shown in Fig. 5A–E, and those in intermittently fluctuating shear rates are shown in Fig. 5F. The total exposure time of shear is $7.2 \times 10^3 \text{ s}$ in Fig. 5A–F. Figure 5A shows HR as a function of the frequency, where the maximum and minimum shear rates are fixed at 300 and 0 s^{-1} , respectively. The

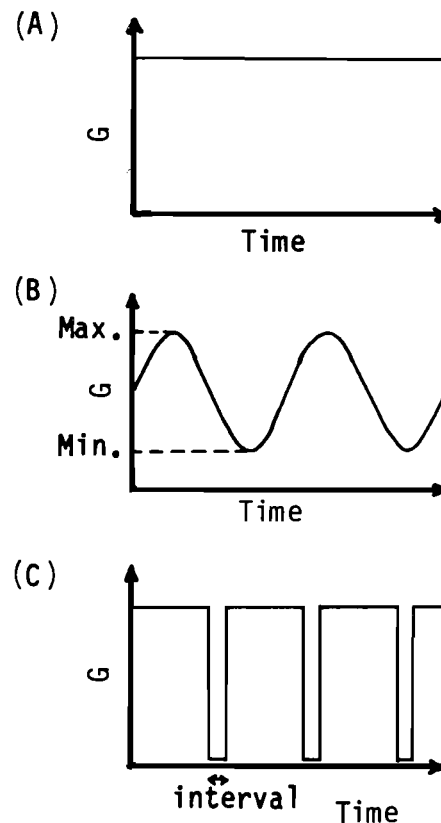


FIG. 4. Mode of fluctuation of shear rate (G). A: Constant. B: Sinusoidal. C: Intermittent.

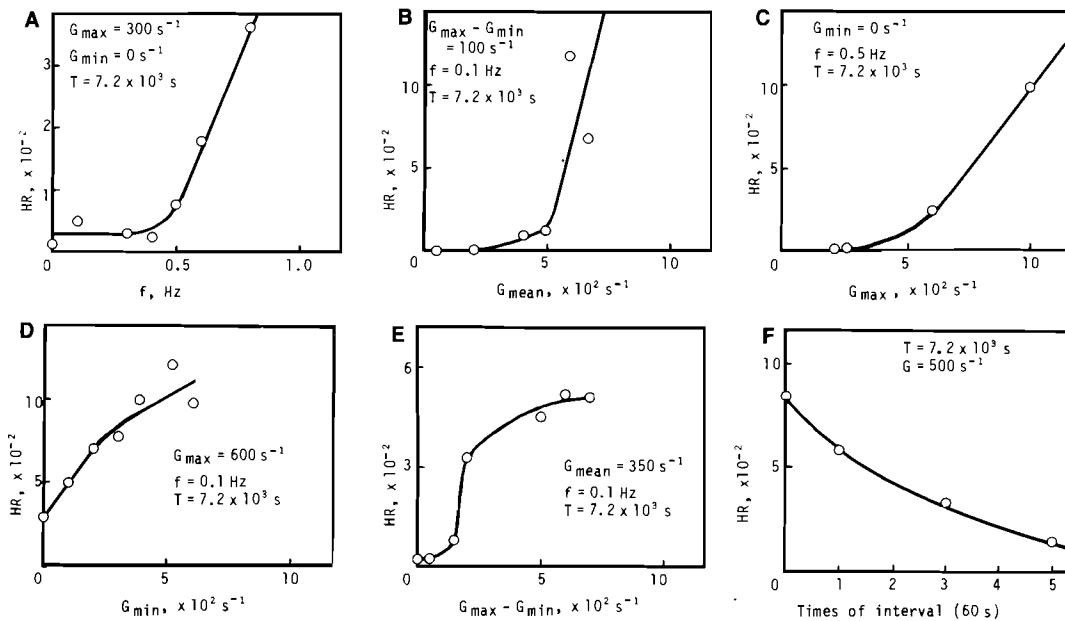


FIG. 5. Hemolysis ratio (HR) as a function of frequency (f) (A), of mean shear rate (G_{mean}) (B), of maximum shear rate (G_{max}) (C), of minimum shear rate (G_{min}) (D), of difference between maximum and minimum shear rates ($G_{max} - G_{min}$) (E) and of times of 60 s intervals (F).

datum point at 0 Hz shows HR at the constant shear rate of 300 s^{-1} . This figure shows that HR increases with a frequency of >0.5 Hz. The following figures (Fig. 5B–E) show HR at the frequency of <0.5 Hz, to keep apart from the effect of the frequency on HR. Figure 5B shows HR as a function of the mean shear rate, where the differences between maximum and minimum shear rates are fixed at 100 s^{-1} and the frequency is a constant of 0.1 Hz . The figure shows that HR becomes large at mean shear rates of $>500 \text{ s}^{-1}$. Figure 5C shows HR as a function of the maximum shear rate, where the minimum shear rate is fixed at 0 s^{-1} and the frequency is 0.5 Hz . This figure shows that HR increases markedly with the maximum shear rate of $>600 \text{ s}^{-1}$. Figure 5D shows HR as a function of the minimum shear rate, where the maximum shear rate is fixed at 600 s^{-1} and the frequency is 0.1 Hz . The datum point at 600 s^{-1} shows HR at the constant shear rate of 600 s^{-1} . This figure shows that HR decreases when the minimum shear rate decreases below 300 s^{-1} . Figure 5E shows HR as a function of the difference between maximum and minimum shear rates, where the mean shear rate is kept at 350 s^{-1} and the frequency is 0.1 Hz . The datum point at 0 s^{-1} shows HR at the constant shear rate of 350 s^{-1} , and the datum point at 700 s^{-1} shows HR when the maximum and minimum shear rates are 700 and 0 s^{-1} , respectively. This figure shows that HR becomes large at the differences between the maximum and minimum shear rates of $>200 \text{ s}^{-1}$; at max-

imum shear rates of $>450 \text{ s}^{-1}$. Figure 5F shows HR as a function of 60 s intervals, when the constant shear rate of 500 s^{-1} is intermittently applied for $7.2 \times 10^3 \text{ s}$ in total. In the case of 3 times a 60 s interval, for example, the exposure time is divided into four parts, and the constant shear rate is applied for $1.8 \times 10^3 \text{ s}$ in each part. This figure shows that HR decreases with increase in interval times.

The hemolysis ratios as a function of the shear exposure time in constant shear rates are shown in Fig. 6A. This figure shows that HR increases markedly above the critical exposure time at each shear rate and that HR is very small (<0.005) even at $1,000 \text{ s}^{-1}$ within 900 s. Data in constant shear rates are summarized in Fig. 6B as a relationship between shear rate and shear exposure time, where HR is 0.01. This figure shows that HR depends on the shear rate and exposure time. Through these tests, HR variations with ϕ are within the range of statistical dispersion, and no apparent morphological change [e.g., fragmentation (3)] is observed with the optical microscope in erythrocytes even when $HR > 0.1$.

DISCUSSION

There have been extensive controlled studies of erythrocyte destruction in flows of various kinematics for over 20 years. Their devices are a concentric cylinder (1), a double-gap concentric cylinder (4), a concentric cylinder with cone and plate at the bot-

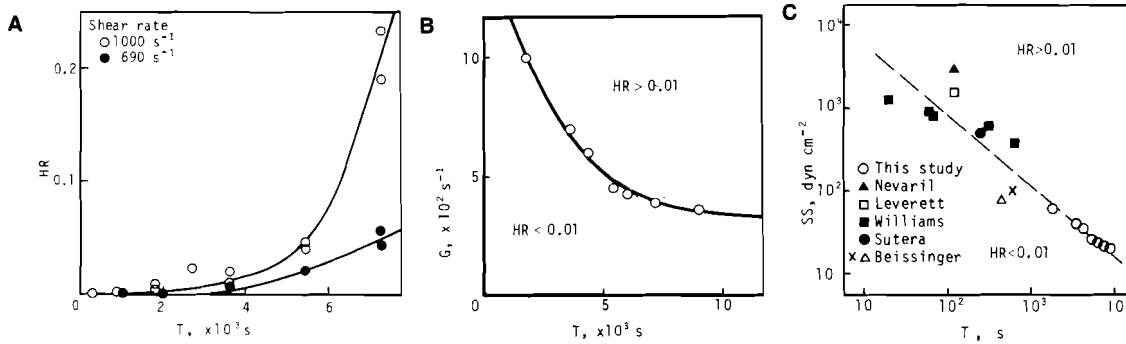


FIG. 6. **A:** Hemolysis ratio (HR) as a function of exposure time (T) in constant shear rates. **B:** Relationship between shear rate (G) and exposure time (T), where hemolysis ratio is 0.01 in constant shear rates. **C:** Relationship between shear stress (SS) and exposure time (T), where hemolysis ratio is 0.01 in constant shear rates. Data taken from this study and from previous studies of Nevaril (13), Leverett (14), Williams (15), Sutera (3), Beissinger (16,5).

tom (5), a cone-and-plate system (6), a system of two parallel horizontal discs (7), a capillary system (8), and a jet injection system (9). The concavo-convex testing machine, which is used in the present study, is a device to form a uniform shear field, and its basic principal is the same as the cone-and-plate system.

This concavo-convex type, however, has some advantages over the cone (with an obtuse apex angle) and plate type; removal of air (10) and collection of the blood sample from the concave cone is easy, and the same shear rate can be exactly applied to the whole blood sample even at the rim (11) of the circular cone (Fig. 3). Shear rates applied in the present study ($<1,000 \text{ s}^{-1}$) are chosen in the range of shear rates of blood flow in the human cardiovascular system (12). This range corresponds to lower shear stresses ($<10^2 \text{ dyn cm}^{-2}$) than those of previous studies (3,5,13–16), in which the higher shear stresses ($>10^2 \text{ dyn cm}^{-2}$) were applied within a short time ($<10^3 \text{ s}$) (Fig. 6C). The exposure time in Fig 5A–F is chosen so that the hemolysis ratio becomes larger than 0.1 at the constant shear rate of $1,000 \text{ s}^{-1}$ (Fig. 6A). The angle between the convex and concave cones (ϕ) has been set so that the rotating speed of the concave cone may not exceed 350 min^{-1} to apply the shear rate (10). In the range of the rotating speed of $<350 \text{ min}^{-1}$, the centrifugal effect is fairly neutralized by the slope of the concave cone so that erythrocytes do not aggregate to the rim of the circular cone.

To apply periodically fluctuating shear rates, the rotating speed of the concave cone is changed sinusoidally in the present study. As a useful dimensionless parameter, the Womersley number (W) has been proposed to estimate the ratio of inertial to viscous forces in periodically fluctuating flows:

$$W = (d/2)\sqrt{2\pi f\rho/\mu} \quad (3)$$

where $d < 0.13 \text{ cm}$ (the distance between the convex and concave cones), $f < 0.5 \text{ Hz}$ (frequency), $\rho = 1 \text{ g/cm}^3$ (density of blood), and $\mu > 0.05 \text{ dyn s cm}^{-2}$ (viscosity of blood at 24°C) in the present tests (shown in Fig 5B–E). Because W is calculated as a smaller value than unity by Eq. 3 [which indicates that inertial forces can be ignored (17)], the flow between the convex and concave cones is estimated to follow the rotary motion of the concave cone.

In the previous study, the author reported that clot growth at foreign surfaces is considerably inhibited at a shear rate of $>400 \text{ s}^{-1}$ (2). Figure 7 shows the relationship between internal radius and flow rate in a cylindrical pipe, where shear rates on its wall are 400 s^{-1} in Poiseuille flow. In this pipe, shear rates of $<400 \text{ s}^{-1}$ are applied to erythrocytes

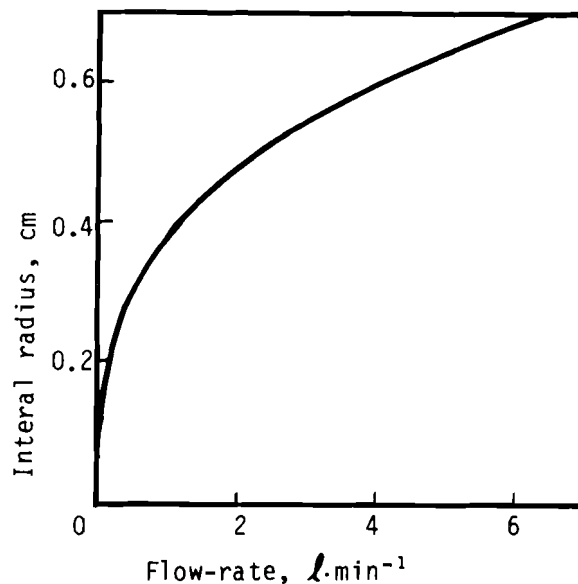


FIG. 7. Relationship between internal radius and flow rate in a cylindrical pipe, where shear rate on its wall is 400 s^{-1} .

because of their aggregation to the axis of the pipe. In the present study, the results show that erythrocyte destruction is considerably inhibited for 7.2×10^3 s at a shear rate of <400 s^{-1} . Thus Fig. 7 suggests an appropriate dimension of artificial blood flow path to inhibit clot growth and mechanical erythrocyte destruction simultaneously, e.g., the appropriate internal radius of the cylindrical pipe, through which 6 ℓ min^{-1} blood flows, is 0.68 cm (where the calculated pressure drop is 4.5 mmHg m^{-1}).

The process of mechanical erythrocyte destruction in blood bulk flow has been considered as follows (Fig. 8). When a shear rate (Fig. 8a) is applied to blood, erythrocytes in blood start to rotate (Fig. 8b). Erythrocytes are deformed from a biconcave to an ellipsoidal shape, and their lines of apsides tilt parallel to the direction of flow (Fig. 8c) (18). Their membranes are then repeatedly stretched in a tank tread-like motion (Fig. 8d) (19,20). When the membranes are destroyed by fatigue through that motion, hemoglobins are released from erythrocytes (Fig. 8e). The destruction of materials by fatigue in general has been experimentally determined by the stress amplitude (S) and the number of the stress cycles (N). In erythrocyte destruction in blood flow, S is governed by the extent of erythrocyte deformation, which is related to the shear rate (G); N is governed by the rotating speed of the tank tread-like membrane motion and by the accumulated number of rotations, where the former is related to the shear rate (G) and the latter is related to the exposure time (T). Figure 9 (calculated from Fig. 6b) shows the relationship between G and $G \times T$, where hemolysis ratio is 0.01 . This figure suggests that erythrocyte membrane is destroyed in fatigue as the above discussion.

The process of mechanical erythrocyte destruction has also been considered in surface interactions (21), which include alteration or denaturation of erythrocyte membrane (by collision or adsorption to the solid surface) and destruction of the membrane during its deformation in the shear field adjacent to the solid surface. One of the methods to evaluate surface interactions is to give variations in materials of solid surface. For this purpose, the sys-

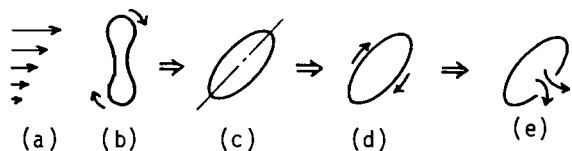


FIG. 8. The process of mechanical erythrocyte destruction in blood bulk flow. See text for details.

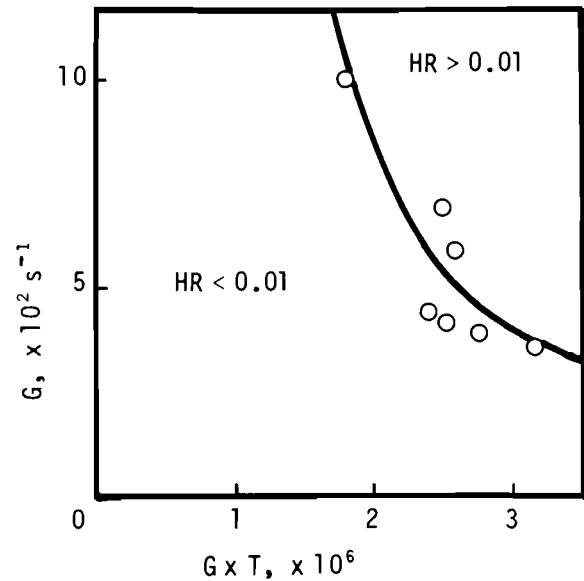


FIG. 9. Relationship between shear rate (G) and product of shear rate (G) and exposure time (T), where hemolysis ratio is 0.01 in constant shear rates.

tem of two parallel horizontal discs (7) and the capillary system (8) are suitable. In the present study, only polymethylmethacrylate has been used because of its transparency and machinability. Another method to evaluate surface interactions is to give variations in surface-to-volume ratio (16). The values of hemolysis ratio independent of ϕ (and surface-to-volume ratio) suggest that the effect of surface interaction on the results of the present study may be minor. The measured order (<4 μm) of surface-roughness of the cones suggests that its effect on the blood flow adjacent to their surfaces may also be minor (11).

In the present study, the results show that the hemolysis ratio increases markedly when the shear rate fluctuates with the maximum of >500 s^{-1} and decreases when the exposure time of larger (>500 s^{-1}) shear rates is interspersed with smaller (<300 s^{-1}) shear rates. These results indicate that the effective part of the exposure time is governed by the threshold of the shear rate and by the viscoelasticity of the erythrocyte membrane (22).

Acknowledgment: The author wishes to express his gratitude for the guidance and encouragement received from Prof. Tadashi Sasada. The author also wishes to express his thanks to Mr. Yohsuke Sugiura, who contributed to this study.

REFERENCES

1. Sutura SP, Croce PA, Mehrjardi M. Hemolysis and subhemolytic alterations of human RBC induced by turbulent

- shear flow. *Trans Am Soc Artif Intern Organs* 1972;18:335-41.
2. Hashimoto S, Maeda H, Sasada T. Effect of shear rate on clot growth at foreign surfaces. *Artif Organs* 1985;9:345-50.
 3. Sutura SP, Mehrjardi MH. Deformation and fragmentation of human red blood cells in turbulent shear flow. *Biophys J* 1975;15:1-10.
 4. Shapiro SI, Williams MC. Hemolysis in simple shear flows. *AIChE J* 1970;16:575-80.
 5. Beissinger RL, Williams MC. Effects of blood storage on rheology and damage in low-stress shear flow. *Biorheology* 1985;22:477-93.
 6. Nanjappa BN, Chang H-K, Glomski CA. Trauma of the erythrocyte membrane associated with low shear stress. *Biophys J* 1973;13:1212-22.
 7. Lampert RH, Williams MC. Effect of surface materials on shear-induced hemolysis. *J Biomed Mater Res* 1972;6:499-532.
 8. Bacher RP, Williams MC. Hemolysis in capillary flow. *J Lab Clin Med* 1970;76:485-96.
 9. Bernstein EF, Marzec UM. Effect of wall interaction, shear stress and osmotic injury on erythrocyte adenosine triphosphate concentration, 2,3 diphosphoglycerate concentration, and the oxyhemoglobin dissociation curve. *Trans Am Soc Artif Intern Organs* 1974;20:47-56.
 10. Lo RK, Nichols AR, Williams MC. Hemolysis artifacts induced in rotating shear devices. *J Biomed Mater Res* 1974; 8:81-6.
 11. Monroe JM, True DE, Williams MC. Surface roughness and edge geometries in hemolysis with rotating disk flow. *J Biomed Mater Res* 1981;15:923-39.
 12. Whitmore RL ed. *Rheology of the circulation*. Oxford: Pergamon Press, 1968;93-6.
 13. Nevaril CG, Lynch EC, Alfrey CP Jr, Hellums JD. Erythrocyte damage and destruction induced by shearing stress. *J Lab Clin Med* 1968;71:784-90.
 14. Leverett LB, Hellums JD, Alfrey CP, Lynch EC. Red blood cell damage by shear stress. *Biophys J* 1972;12:257-73.
 15. Williams AR. Viscoelasticity of the human erythrocyte membrane. *Biorheology* 1973;10:313-9.
 16. Beissinger RL, Williams MC. A dual mechanism for low-stress hemolysis in laminar blood flow. *AIChE J* 1984;30: 569-77.
 17. Caro CG, Pedley TJ, Schroter RC, Seed WA, eds. *The mechanics of the circulation*. Oxford: Oxford University Press, 1978;57-60.
 18. Schmit-Schönbein H, Wells R. Fluid drop-like transition of erythrocytes under shear. *Science* 1969;165:288-91.
 19. Fischer TM. On the energy dissipation in a tank-treading human red blood cell. *Biophys J* 1980;32:863-8.
 20. Niimi H, Sugihara M. Cyclic loading on the red cell membrane in a shear flow: a possible cause of hemolysis. *J Biomech Eng (Trans ASME)* 1985;107:91-5.
 21. Keller KH. The dynamics of the interaction of cells with surfaces. In: Salzman EW, ed. *Interaction of the blood with natural and artificial surfaces*. New York: Marcel Dekker, 1981:119-38.
 22. Rand RP. Mechanical properties of the red cell membrane. *Biophys J* 1964;4:303-16.